

Multifunctional Polyurethane Network Structures

Jeffrey J. Fedderly*, Gilbert F. Lee, John D. Lee, Bruce Hartmann
Naval Surface Warfare Center, Carderock Division, 9500 MacArthur
Boulevard, West Bethesda, MD 20817-5700, USA
FedderlyJJ@nswccd.navy.mil

Karel Dušek, Ján Šomvářsky, and Miroslava Smrčková
Institute of Macromolecular Chemistry, Heyrovského nam. 2, 16006 Prague 6,
Czech Republic

ABSTRACT: A series of thirteen polyurethanes were synthesized using blends of monofunctional, difunctional, and trifunctional poly(propylene oxides) reacted with 4,4'-diphenylmethane diisocyanate in a stoichiometric ratio. Experimental measurements were made of glass transition temperature, sol fraction, and dynamic mechanical properties. Computer simulations based on the theory of branching processes were made on the same systems. The glass transition temperature was correlated with the number average functionality of the components. Dynamic mechanical data was fitted to the Havriliak-Negami model. A correlation was demonstrated between the measured rubbery modulus and the concentration of elastically active network chains.

1. Introduction

Polyurethanes are often copolymers of difunctional polyols reacted with difunctional isocyanates. In many cases, however, trifunctional polyols or trifunctional isocyanates are added to result in a crosslinked polymer with a network structure. A traditional approach to studying network properties would involve blending a trifunctional polyol at various levels into a formulation with a difunctional polyol and a diisocyanate. From this, one could study the effect of network structure on physical properties. In the present effort, a series of polyurethanes was made in which trifunctional polyols were blended with monofunctional alcohols and then reacted with a diisocyanate. In addition, some samples were made which incorporated mono-, di-, and trifunctional polyols. In this manner, the effect of monofunctionality on network structure and physical properties could be determined. The polyols used in this study were hydroxyl-terminated poly(propylene oxides). The polyols were reacted with diphenylmethane diisocyanate (MDI) to form polyurethanes. Each functional material (mono-, di, and triol) was selected to have a nominal equivalent weight of 500. Therefore, no matter in what ratio the polyols were blended, the resulting polymers would have the same urethane content, the same aromatic content, and the same propylene oxide content. In our earlier study ¹⁾ using monofunctional polyols, the urethane content changed when

the monofunctional content changed, making it difficult to separate effects. In the present study, the only differences among the polymers are their network structure. Polymers with trifunctional and monofunctional polyols have branch points and significantly more chain ends than are present in linear polymers formed from purely difunctional polyols. This study will determine how these differences affect glass transition temperature, sol fraction, and dynamic mechanical properties. Comparisons of the polymers synthesized with various functionalities will be made at constant number average functionality, F_n , given by

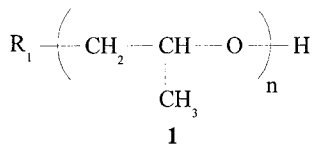
$$F_n = \sum n_i F_i / \sum n_i \quad (1)$$

where n_i is the number of moles of the i^{th} component and F_i is the functionality of the i^{th} component.

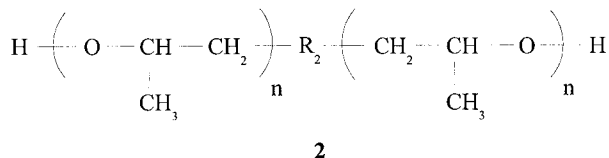
2. Experimental Procedures

2.1 Sample preparation

Polyurethane samples were prepared by reacting hydroxy-terminated poly(propylene oxides) (PPOs) of various functionality with diphenylmethane diisocyanate (MDI). The PPOs used had nominal functionalities of one, two, and three. The PPOs were chosen to have a nominal equivalent weight of 500 g/eq. The monofunctional material (1F) has structural formula **1**.



The difunctional material (2F) has structural formula **2**.



The trifunctional material (3F) has structural formula **3**.

2.3 Determination of sol fraction

Sol fractions were measured from 10 mm by 20 mm specimens cut from 2 mm thick sheets. Samples were weighed dry in a dry room with relative humidity less than 0.25 percent, then immersed in sealed jars containing nominally 40 grams of 2-methoxyethyl ether as solvent. After two days the samples were transferred to jars containing fresh solvent and kept for an additional six days. The samples were then removed from the solvent, quickly blotted dry and re-weighed in the dry room.

2.4 Determination of dynamic mechanical properties

The dynamic mechanical properties were measured using a resonance technique developed at this laboratory ²⁾. This technique has been used in a number of studies on polymer properties ^{1,3,4)}. The apparatus is based on producing resonance in a bar specimen. Typical specimen length is 10-15 cm with square lateral dimensions of 0.635 cm. Measurements are made over 1 decade of frequency in the kHz region from -60 to 70°C at 5 degree intervals. By applying the time-temperature superposition principle, the raw data are shifted to generate a reduced frequency plot (over as many as 20 decades of frequency) at a constant reference temperature.

In brief, an electromagnetic shaker is used to drive a test specimen at one end while the other end is allowed to move freely. Miniature accelerometers are adhesively bonded on each end to measure the driving point acceleration and the acceleration of the free end. The output signals from the accelerometers are amplified and routed to a dual channel Fast Fourier Transform spectrum analyzer. The analyzer digitizes the measured signals. To increase the signal to noise ratio, the analyzer performs a minimum of 32 time averages. The analyzer displays the signals as amplitude and phase of the acceleration ratio over the frequency range from 25 to 50,000 Hz.

At certain frequencies, the amplitude of the acceleration ratio goes through local resonant peaks occurring in the kHz region. The resonant peaks are spread out over a frequency range of about one and a half decades. The number of resonant peaks that can be measured is dependent on the modulus and loss factor of the material, but, typically, there are three to six peaks.

3. Polymers Synthesized

The set of polymers synthesized for this work are listed in Table 1, where the functionalities of the poly(propylene oxide) components used are listed as the Type of polymer as well as the number average functionality of the resulting polymer and the number of moles of each of the three functionalities used in the synthesis. N_{XF} is the molar fraction of the X-functional polyol in the polyol blends.

Table 1. Polymer set synthesized, polymer density, and glass transition temperature

Type	F_n	N_{1F}	N_{2F}	N_{3F}	$\rho/(\text{cm}^3/\text{g})$	$T_g/^\circ\text{C}$
2F	1.99		1.000		-	-28.6
1F+3F	1.99	0.500		0.500	1.072	-
2F+3F	2.12		0.867	0.133	1.076	-28.3
F+2F+3F	2.12	0.217	0.434	0.349	1.075	-
1F+3F	2.12	0.434		0.566	1.072	-27.9
2F+3F	2.20		0.786	0.214	1.074	-26.9
F+2F+3F	2.20	0.196	0.393	0.411	1.075	-
1F+3F	2.20	0.393		0.607	1.077	-29.0
2F+3F	2.40		0.582	0.418	1.078	-25.1
1F+3F	2.40	0.291		0.709	1.081	-25.9
2F+3F	2.60		0.378	0.622	1.081	-25.4
1F+3F	2.60	0.189		0.811	1.081	-23.9
3F	2.97			1.000	1.082	-22.9

4. Glass Transition Temperature

As all of the polymers synthesized here are very similar in overall composition, their glass transition temperatures are very similar, varying by only six degrees among the 13 polymers. The glass transition temperatures are given in Table 1. There is, however, a general trend that the glass transition temperature increases as a function of number average functionality, as shown in Figure 1. Thus, crosslinking tends to increase the glass transition temperature, but this effect is seen to be relatively small compared with changes in glass transition temperature resulting from changes in chemical composition, urethane concentration, for example.

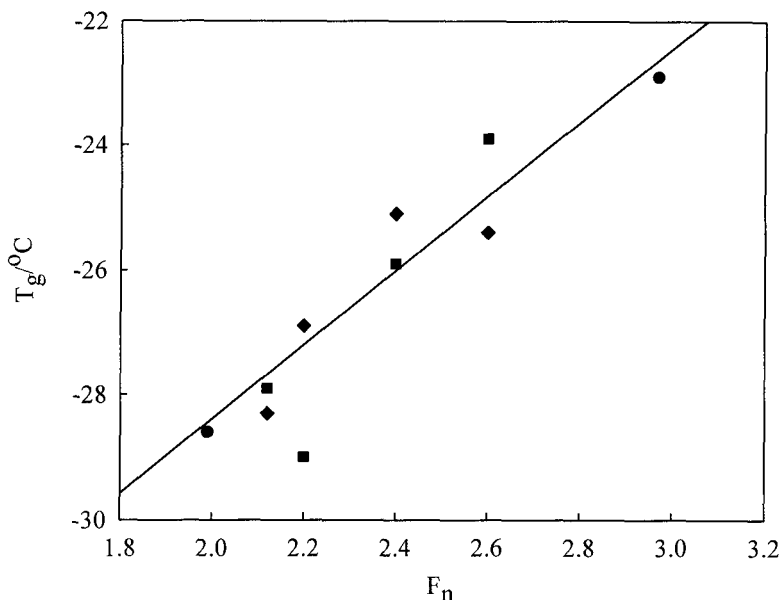


Figure 1. Glass transition temperature as a function of number average functionality.

● = pure 2F and pure 3F, ■ = 2F+3F, and ◆ = 1F+3F

5. Sol fraction

In the comparison of the typical crosslinked polyurethanes (2F+3F) to the novel construction using monofunctional reactants (1F+3F), it was expected that the 2F+3F materials would have very low sol fractions, whereas the 1F+3F materials would have considerable sol fractions. The existence of sol in these materials might have a substantial impact on various properties. The measured sol fractions are listed in Table 2. For the given polyol functionalities the 1F+3F materials had two to three times the sol fraction as the 2F+3F materials. Although the 2F+3F materials had low sol fractions, they were not as low as expected; for full conversion of functional groups almost no sol fraction should be present. This indicated that imperfections occurred during polymerization. These could be due to incomplete conversion, inexact stoichiometry of the polyols to isocyanate, cyclization or other side reactions. The most straightforward approach was to attribute the additional sol to incomplete conversion. Therefore, in the network calculations to follow, the sol fraction was used to predict the degree of conversion. The various network properties were then based on this conversion.

Table 2. Network parameters.

Type	F_n	W_s	α	W_e	M_{ns}	W_d	M_{nd}	N_e	v_e $\times 10^4$
1F+3F	1.99	0.244	0.939	0.253	1600	0.503	3575	0.039	0.881
2F+3F	2.12	0.070	0.977	0.539	7680	0.391	8923	0.035	0.627
1F+2F+3F	2.12	0.199	0.943	0.304	2840	0.497	4897	0.035	0.727
1F+3F	2.12	0.122	0.959	0.420	1310	0.458	2460	0.097	1.834
2F+3F	2.20	0.040	0.971	0.638	4790	0.322	5085	0.070	1.191
1F+2F+3F	2.20	0.119	0.947	0.425	2310	0.456	3514	0.068	1.254
1F+3F	2.20	0.087	0.962	0.493	1220	0.420	2150	0.132	2.356
2F+3F	2.40	0.017	0.960	0.744	2490	0.238	2392	0.159	2.545
1F+3F	2.40	0.041	0.963	0.630	1060	0.330	1682	0.212	3.477
2F+3F	2.60	0.007	0.958	0.818	1620	0.174	1481	0.259	3.972
1F+3F	2.60	0.022	0.953	0.714	980	0.265	1388	0.271	4.211
3F	2.97	0.003	0.942	0.846	860	0.150	909	0.386	5.567

F_n is the number average functionality of the polyol blend, W_s , W_e , and W_d represent the weight fractions of the sol, elastic, and dangling chain portions of the polymer respectively, M_{ns} and M_{nd} represent the number average molecular weights of the sol and dangling chains, N_e represents the number of elastically active network chains, and v_{ev} represents the concentration of elastically active network chains in moles per cm^3 .

6. Network Calculations

To understand better the nature of these polymer systems, predictions of various network properties were made. To accomplish this, computer simulations were performed using the theory of branching processes based on generation of structures from component units in different reaction states ⁵⁾. The simulations predict gel point and several properties as a function of conversion, including: molecular weight, sol-gel fractions and their molecular weights, dangling chain fractions and their molecular weights ⁶⁾, and number of elastically active network chains (EANC).

A detailed derivation of the theoretical relations will be published later. From the number of EANCs the concentration of EANCs per unit volume (v_{ev}) can be calculated.

$$v_e = N_e \rho / M_n w_g \quad (2)$$

where N_e is the ratio of the number of moles of EANC to the number of moles of starting materials, ρ is the polymer density, M_n is the number average molecular weight of the starting materials, and w_g is the weight fraction of gel. The importance of this quantity is that theory relates this parameter to the rubbery modulus of the polymer, and this correlation will be demonstrated below. During the polymerization of the system a gel point is reached at a critical conversion. Before this point all of the material is soluble, or sol. Beyond this point, sol begins to reduce as material forms into a network structure. The growth of the network is monitored by following the increase in the number of EANCs (N_e) as a function of conversion. A plot of N_e versus conversion for the 2F+3F series of polymers is shown in Figure 2.

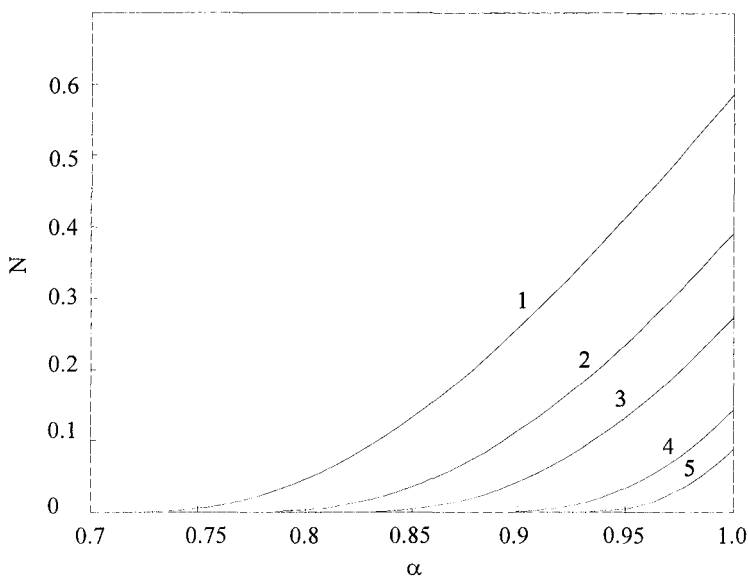


Figure 2. Number of elastically active network chains as a function of conversion for 2F+3F polymers. 1 = F2.97, 2 = F2.60, 3 = F2.40, 4 = F2.20, 5 = F2.12.

Figure 3 shows the predicted sol fraction as a function of conversion for the 2F+3F materials. The measured sol values are greater than the near zero values for conversions approaching unity. Therefore, network properties were determined for conversions corresponding to the measured sol fractions. The values of various network properties are listed in Table 2.

As one diverges from the 3F material (the limiting value for both the 1F+3F and 2F+3F series), towards lower functionality, several comparisons between the materials can be made. For a given functionality, the concentration of EANC for the 1F+3F is twice as

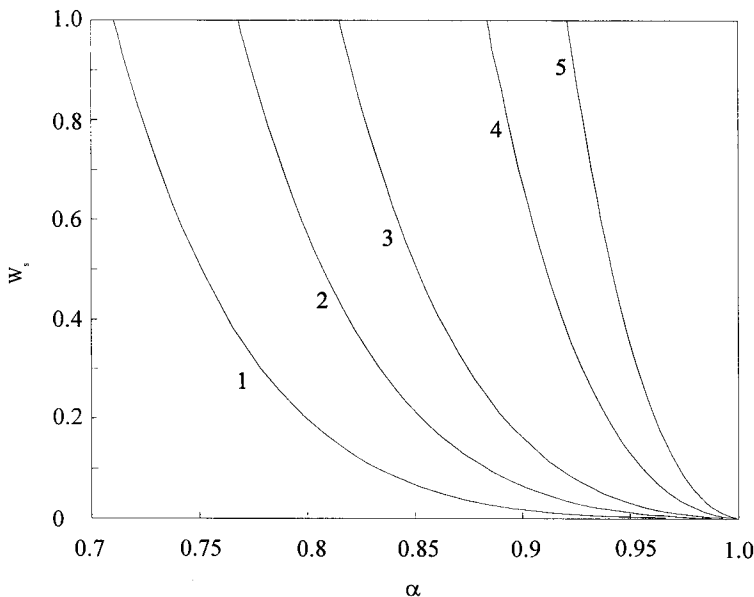


Figure 3. Sol Fraction as a function of conversion for 2F+3F polymers. 1 = F2.97, 2 = F2.60, 3 = F2.40, 4 = F2.20, 5 = F2.12.

large as for the 2F+3F. The weight fraction elastic portion of the 2F+3F material, however, is significantly higher. From this, though not explicitly calculated, the molecular weight of the EANCs for the 2F+3F are obviously significantly greater than for the 1F+3F material. The weight fraction of the dangling chains are greater for the 1F+3F material, but the molecular weight of dangling chains of the 2F+3F material is two and a half times greater than for the 1F+3F material. The weight fraction of the sol is twice as great for the 1F+3F as for the 2F+3F material. The molecular weight of the sol for the 2F+3F is four times as great as for the 1F+3F. This is due to the fact that the sol fraction of 1F+3F material is predominantly composed of the reacted 1F chains and therefore the gel contains more branch points; this is the reason for its higher crosslinking density compared to 2F+3F materials.

7. Dynamic Mechanical Properties

The dynamic mechanical results were fitted to the Havriliak-Negami (HN) dispersion relation ⁷⁾

$$\frac{G^* - G_\infty}{G_0 - G_\infty} = \frac{1}{[1 + (i f / f_0)^\alpha]^\beta} \quad (3)$$

where G_{∞} is the limiting high frequency modulus (glassy modulus), G_0 is the limiting low frequency modulus (rubbery modulus), f is the frequency of the measurement, f_0 is the dominant relaxation frequency, α is a parameter governing the width of the transition, and β is a parameter governing the asymmetry of the transition. Both α and β are dimensionless parameters with values between zero and one. The relaxation frequency f_0 is related to the location of the glass transition.

A typical master curve is shown in Figure 4. The symbols represent the measured

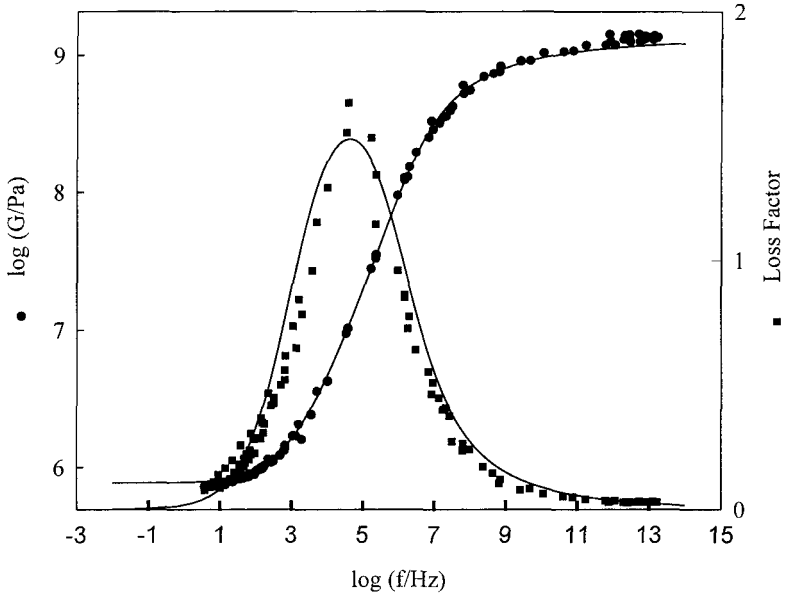


Figure 4. Master curves for 1F+3F F2.40.

(shifted) data and the solid lines are non-linear least square curve fits to the HN equation. The HN parameters G_0 and G_{∞} are listed in Table 3 along with the loss factor peak height, width, and maximum position. The width values represent the full width of the loss peak, in decades of frequency, at half height.

A number of observations can be made from the dynamic mechanical data. The position of the loss peaks, $\log(f_{\max})$, all fall within a very tight range (3.9 to 4.8). This

Table 3. Dynamic Mechanical Parameters

Type	F_n	$\log(f_{\max})$	G_0/MPa	G_∞/GPa	Height	Width
2F	1.99	-	-			
1F+3F	1.99	4.50	0.154	1.16	1.23	5.89
2F+3F	2.12	4.80	0.436	0.81	1.23	4.53
1F+2F+3F	2.12	4.06	0.292	1.61	1.77	3.96
1F+3F	2.12	3.91	0.348	1.64	2.08	3.43
2F+3F	2.20	4.56	0.735	1.55	1.37	4.06
1F+2F+3F	2.20	4.07	0.423	1.29	2.19	3.30
1F+3F	2.20	4.49	0.461	1.16	1.42	4.38
2F+3F	2.40	4.80	1.02	1.07	1.48	3.73
1F+3F	2.40	4.62	0.769	1.30	1.49	3.82
2F+3F	2.60	4.62	1.15	1.33	2.28	2.64
1F+3F	2.60	4.23	1.03	1.38	2.25	2.74
3F	2.97	4.55	1.68	1.55	2.13	2.30

was to be expected. The transition that is observed in the dynamic mechanical data is due to the glass transition. Therefore, the position of the loss peak correlates with the glass transition temperature. The T_g s only had a range of 6 °C, thus, it is consistent that the loss peaks are closely spaced. The G_∞ values are also very similar to each other with an average value of 1.3 GPa. Thus, variations in network structure have little effect on the glassy state. All of the materials have very high loss factors, ranging from 1.2 to 2.3. There is a general trend for the height to increase as the functionality increases from two to three. As expected ⁴⁾, there is an inverse trend with peak width. Thus, peaks are either tall and narrow or short and broad.

In Figure 5 we show the width of the loss factor peak versus the dangling chain molecular weight. Dangling chains (and the sol) represent slowly relaxing substructures of the network. The width generally increases with the molecular weight (and their weight fraction) of the dangling chains and sol. The behavior of the 1F+3F series is different from that of the 2F+3F and 1F+2F+3F series. This may be because the dangling chains in the 1F+3F series are mostly linear, whereas the chains are branched in the 2F+3F series.

The most significant dynamic mechanical property to exhibit a dependence on network structure is the rubbery modulus, G_0 . As can be seen in Figure 6, all three series exhibit

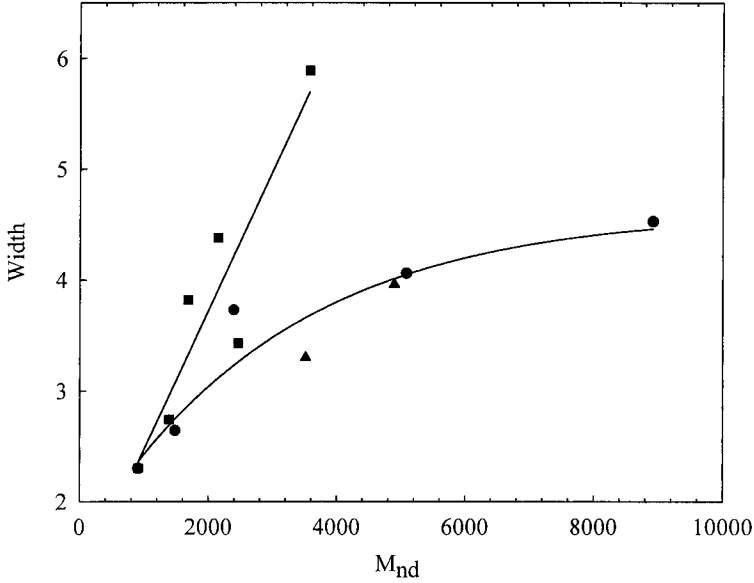


Figure 5. Loss factor peak width as a function of the molecular weight of dangling chains. ■ = 1F+3F polymers, ● = 2F+3F polymers, ▲ = 1F+2F+3F polymers.

a linear dependence on the concentration of EANCs, with each type having a distinct slope. All three curves converge at the 3F material which is the endpoint of all three series. The 1F+3F series has the greatest slope and appears to be converging closely towards zero modulus for zero EANC concentration. The 2F+3F series has the least dependence on EANC concentration and appears to be converging towards a modulus of approximately 0.7 MPa. It must be noted, however, that a sample of pure difunctional material producing linear chains only was made, but was unable to be measured. It flowed and was extremely soft. The 1F+2F+3F series exhibits intermediate properties.

The dependence on EANC concentration is predicted to be linear within a certain range of concentrations of EANCs. However, often this dependence does not extrapolate to a zero value of G_0 at the gel point because of the trapped entanglements contribution:

$$(v_{ev})_{exp} = (v_{ev})_{chem} + (v_{ev})_{ent} \quad (4)$$

where the subscript $_{\text{chem}}$ refers to EANCs due to chemical crosslinks and $_{\text{ent}}$ to the trapped entanglement contribution. The 1F+3F materials have much higher fraction of “inert” material (dangling chains) which “dilute” the EANCs backbones. Alternatively, one can say that the dangling chains make the EANCs more bulky. It is known increasing amount of diluent or increasing bulkiness of the chains reduces the number of entanglements. Therefore, the contribution of trapped entanglements to modulus for the 1F + 3F materials is negligible.

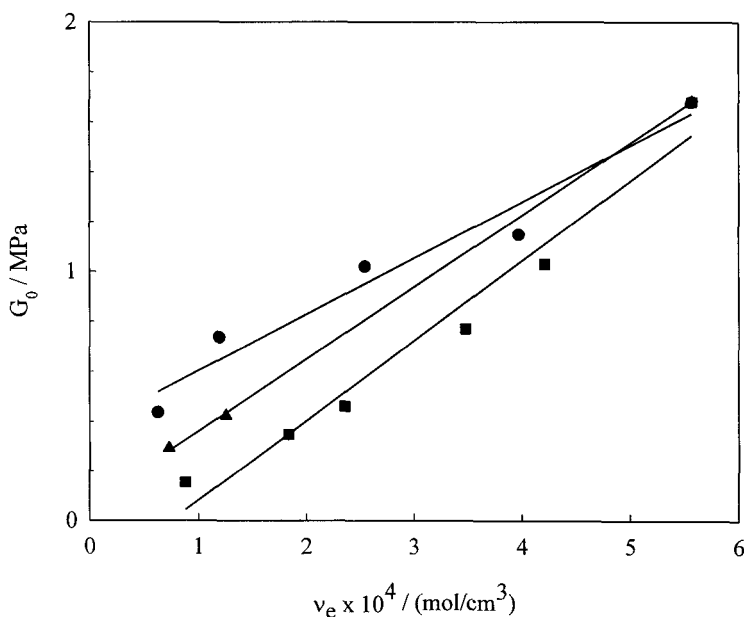


Figure 6. Rubbery modulus as a function of the concentration of elastically active network chains. \blacksquare = 1F+3F polymers, \bullet = 2F+3F polymers
 \blacktriangle = 1F+2F+3F polymers

8. Concluding Remarks

A series of thirteen polyurethane samples were synthesized, incorporating combinations of mono-, di-, and tri-functional components with number average functionalities ranging from 1.99 to 2.97. The polymers were carefully chosen so that the urethane content, aromatic content, and overall composition was the same in all the polymers.

They differed only in their network structure. Calculations were made of the network structures of these polymers using the theory of branching processes and measurements were made of the glass transition temperature, sol fraction, and dynamic mechanical properties. Based on these results, the following conclusions were reached:

Glass transition temperatures correlate with number average functionality, though the variation is small compared with variations resulting from composition changes such as urethane content.

Sol fraction is greater in the 1F+3F polymers than in the 2F+3F polymers. The measured sol fraction can be used to estimate the degree of conversion.

With regard to dynamic mechanical properties, it is observed that the location of the loss factor peak shows very little variation, in agreement with the small spread in the glass transition temperatures. The glassy modulus is nearly the same for all the polymers, showing that network structure does not have a significant effect on glassy state properties. The height and width of the loss factor peak are correlated and the width is correlated with molecular weight of the dangling chains.

The most significant effect of network structure on dynamic mechanical properties is found with the rubbery modulus. It was shown that the rubbery modulus correlates with the concentration of elastically active network chains with 1F+3F materials having significantly different slopes than 2F+3F materials. This is due to the much lower number of trapped entanglement in the 1F+3F materials.

Acknowledgements

Supported by NATO, Brussels, Belgium under Collaborative Research Grant CRG 970041, by the In-house Laboratory Independent Research Program of NSWCCD, West Bethesda, MD, USA, and by Grant Agency of the Academy of Sciences of the Czech Republic, Grant No. A4050808.

References

1. J. J. Fedderly, G. F. Lee, D. J. Ferragut, and B. Hartmann, *Polymer Eng. Sci.* **36**, 1107 (1996)
2. W. M. Madigosky and G. F. Lee, *J. Acoust. Soc. Amer.* **73**, 1374 (1983)
3. B. Hartmann and G. F. Lee, *J. Non-Cryst. Solids* **131-133**, 887 (1991)
4. B. Hartmann, G. F. Lee, and J. D. Lee, *J. Accost. Soc. Am.* **95**, 226 (1994).
5. K. Dusek, in *Telechelic Polymers: Synthesis and Application*, E. J. Goethals, Ed., CRC Press, Boca Raton, FL, pp 289-360 (1989)
6. K. Dusek and M. Ilavský, *Progr. Coll. Polym. Sci.* **80**, 26 (1989)
7. S. Havriliak and S. Negami, *J. Polymer Sci. C* **14**, 99 (1966)